

Laser Light-Scattering Characterization of the Molecular Weight Distribution of Dextran

Chi Wu

Department of Chemistry, The Chinese University of Hong Kong, Shatin, N.T., Hong Kong, China

Received December 9, 1992

ABSTRACT: Laser light scattering (LLS) including the angular dependence of the absolute integrated scattered intensity (static LLS) and of the line-width distribution (dynamic LLS) has been used to characterize the molecular weight distributions of dextran samples with different branching densities. In the process of converting a translational diffusion coefficient distribution ($G(D)$) obtained from the precisely measured intensity-intensity time correlation function into a molecular weight distribution (MWD), we encountered the following two problems: the change of the dextran conformation as a function of molecular weight and the lack of a set of narrowly distributed dextran standards. A procedure to solve these two problems simultaneously has been presented, wherein the weight-average molecular weight (M_w) obtained from static LLS is used to constrain the conversion of $G(D)$ to MWD. By using this procedure, we were able to obtain a calibration of D (cm^2/s) = $1.98 \times 10^{-4} M^{-[0.857-0.0201 \log(M)]}$ with a set of *broadly* distributed dextrans and to accomplish the calculation of MWD of dextran from the measured spectral distribution. The calculated molecular weight distributions are fairly comparable to the ones obtained from gel filtration experiments.

1. Introduction

Dextran is a high molecular weight branched polysaccharide synthesized from sucrose by bacteria.¹ This polymer consists of anhydroglucose repeat units joined by α -acetal linkages. Approximately 95% of those linkages are through carbons 1 and 6 in the main and branch chains and the rest of them are between carbons 1 and 3 at the branching point.^{2,3} Dextran is used as a partial substitute for blood plasma, mainly as a volume expander. Its pharmacological applications are directly related to its physicochemical properties. Normally, the dextran produced by industrial fermentation has to be partially hydrolyzed and then fractionated in order to give a dextran with a certain molecular weight distribution (MWD) which is suitable for clinical use.⁴ Therefore, the accurate determination of MWD of a given dextran is often important in its applications.

In the past, many methods, such as the classic fractionation (i.e., precipitation, extraction, ultrafiltration, etc.),⁵ size-exclusion chromatography (SEC),⁶ and ultracentrifuge,⁷ have been used to determine the average molecular weight or MWD of dextran. The fractionation normally involves a time-consuming process and its resolution is limited. In the case of SEC, the axial dispersion of dextran, coexistence of adsorption (dextran is a polar system), and calibration (using a set of narrowly distributed standard dextran standards fractionated from the same kind of dextran and performing in identical experimental conditions) are the main difficulties. When using ultracentrifuge, the analysis of dextran in water is hindered by the large deviation from ideality. Only an apparent distribution of the sedimentation coefficient can be obtained, even at high dilution, which means that the real distribution has to be calculated by extrapolating the apparent boundary spreading of velocities to infinite dilution. This extrapolation usually introduces some inaccuracies in the final molecular weight distribution.

Light scattering as a well-established analytical method has been extensively used to determine the weight-average molecular weight of various polymer samples including dextran.⁸⁻¹⁰ At the present time, due to the advances of laser as the light source, photomultiplier, correlator, and computer in the past 20 years, we are able to measure not

only the average scattering intensity (static light scattering) but also the fluctuations of the scattered light (dynamic light scattering). Various computer programs have been developed to make a Laplace inversion of the measured correlation function in order to give an approximated characteristic line-width distribution, $G(\Gamma)$,¹¹⁻¹⁴ which can be further reduced to a translational diffusion coefficient distribution ($G(D)$) or even to a molecular weight distribution (MWD) if the calibration between D and M is known.^{15,16} As an absolute analytical method, using laser light scattering (LLS) to determine MWD has certain advantages over the other analytic techniques. For example, the calibration between D and M is independent of the particular LLS instrument.

The present work serves two purposes. One is to determine MWD of dextran for the first time by only using LLS. The other is to present a LLS data analysis procedure of using a set of *broadly* distributed samples to establish a calibration between D and M for some special polymers, such as dextran, whose D cannot be scaled to M as $D = k_D M^{-\alpha_D}$ with only two scaling constants k_D and α_D .

2. Basic Theories

Static Light Scattering. The angular dependence of the excess absolute time-averaged scattered intensity, known as the excess Rayleigh ratio [$R_{vv}(\theta)$], was measured. For a dilute polymer solution at concentration C (g/mL) and scattering angle θ , $R_{vv}(\theta)$ can be approximately expressed as¹⁷

$$\frac{KC}{R_{vv}(\theta)} \cong \frac{1}{M_w P(\theta)} + 2A_2 C \quad (1)$$

where $K = 4\pi^2 n^2 (\partial n / \partial C)^2 / (N_A \lambda_0^4)$ and $q = (4\pi n / \lambda_0) \sin(\theta/2)$ with N_A , n , and λ_0 being Avogadro's number, the solvent refractive index, and the wavelength of light in vacuo, respectively. If the root-mean-square z -average radius, $\langle R_g^2 \rangle_z^{1/2}$, is smaller than q^{-1} , $1/P(\theta)$ can be approximated as $(1 + 1/3 \langle R_g^2 \rangle_z q^2)$. By measuring $R_{vv}(\theta)$ at a set of C and θ , we can determine M_w , $\langle R_g^2 \rangle_z^{1/2}$, and A_2 from a Zimm plot which incorporates θ and C extrapolations on a single grid.¹⁸ Figure 1 shows a typical Zimm plot of dextran in water at 25 °C.

Dynamic Light Scattering. An intensity-intensity time correlation function $G^{(2)}(n\delta\tau, \theta)$ in the self-beating mode

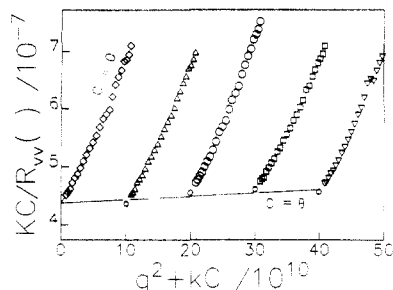


Figure 1. Typical static Zimm plot of dextran T2000 measured in water at $T = 25^\circ\text{C}$; where C ranges from 1 to 3×10^{-4} g/mL.

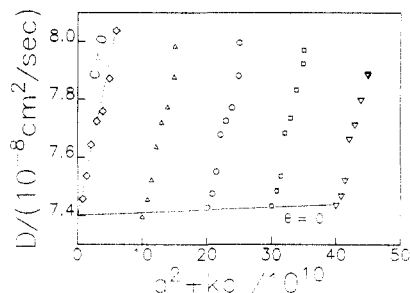


Figure 2. Typical dynamic Zimm plot of dextran T2000 measured in water at 25°C , where C ranges from 1 to 3×10^{-4} g/mL.

is normally measured, which has the following form^{18,19}

$$G^{(2)}(n\delta\tau, \theta) = \langle I(n\delta\tau, \theta) I(0, \theta) \rangle = A[1 + \beta |g^{(1)}(n\delta\tau, \theta)|^2] \quad (2)$$

where A is a measured base line, β is a parameter depending on the coherence of the detection, n is the channel number, $\delta\tau$ is the sample time, and $g^{(1)}(n\delta\tau, \theta)$ is the normalized first-order electric field time correlation function. In our correlation function measurements, instead of using A as an adjustable parameter, we insisted on having A and $\lim_{n \rightarrow \infty} G^{(2)}(n\delta\tau, \theta)$ (the calculated base line) agree to within 0.1%. For a polydisperse sample, $g^{(1)}(n\delta\tau, \theta)$ is related to $G(\Gamma)$ by

$$g^{(1)}(n\delta\tau, \theta) = \langle E(n\delta\tau, \theta) E^*(0, \theta) \rangle = \int_0^\infty G(\Gamma) e^{-\Gamma n\delta\tau} d\Gamma \quad (3)$$

The mostly accepted analysis program CONTIN,¹² which was kindly furnished by S. W. Provencher, was used in the present work to calculate $G(\Gamma)$ from the measured $G^{(2)}(n\delta\tau, \theta)$. It should be noted that Γ normally depends on both concentration and scattering angle. The increasing interaction between polymer molecules as a function of concentration will effect the diffusion process. This effect can be expressed as a linear function of concentration in a dilute solution. At higher scattering angle, Γ usually contains some contributions from the internal molecular motions. Those effects can be expressed in the equation²⁰

$$\Gamma/q^2 = D(1 + k_d C)(1 + f \langle R_g^2 \rangle q^2) \quad (4)$$

where k_d is the diffusion second virial coefficient which is related to both the hydrodynamic and thermodynamic effects and f is a dimensionless number which depends on chain structure, polydispersity, and solvent quality. Theoretically, f is between 0 and $1/3$. It is also known that branching generally reduces f because this structure gradually approaches the homogeneous sphere behavior with increasing branching density.²⁰ D , k_d , and f can be obtained from a Zimm plot similar to that in static LLS. Figure 2 shows a typical plot of $\bar{\Gamma}/q^2$ versus both C and q^2 , where $\bar{\Gamma} = \int_0^\infty G(\Gamma) \Gamma d\Gamma$.

Transformation of $G(D)$ to MWD. The key problem is how to establish a calibration between D and M . In the

past, various methods have been used to solve this problem: such as measuring D and M of many narrowly distributed standards;²¹ using $G(D)$ and M_w of at least two broadly distributed samples and assuming polymer conformation is not a function of M ;¹⁶ estimating the calibrating constant from other experimental results (for example, from polymer conformation, solvent quality, and viscosity data);²² and combining the elution volume distribution ($C(V)$) of a broadly distributed sample from SEC with both $G(D)$ and M_w from laser light scattering.¹⁵

After having the calibration, $G(D)$ can be transferred to MWD according to the following principles: as $C \rightarrow 0$ and $\theta \rightarrow 0$, based on eqs 1 and 3, we have

$$\int_0^\infty G(D) dD = \gamma \int_0^\infty F_n(M) M^2 dM \quad (5)$$

where γ is a normalization constant and $F_n(M)$ is a number distribution. Equation 5 can be rewritten as

$$\int_0^\infty G(D) \frac{dD}{dM} dM = \gamma \int_0^\infty F_n(M) M^2 dM \quad (6)$$

By comparing both sides of eq 6, we have

$$F_w(M) = F_n(M) M \propto \frac{G(D)}{M} \frac{dD}{dM} \quad \text{or} \quad F_n(M) \propto \frac{G(D)}{M^2} \frac{dD}{dM} \quad (7)$$

where $F_w(M)$ is a weight distribution and all proportional constants have been omitted since they are irrelevant to both distributions. For a given calibration between D and M , we can first calculate both M and dD/dM and then $F_w(M)$ or $F_n(M)$ according to eq 7.

3. Experimental Methods

Preparation of Solutions. The dextrans (T10, T40, T70, T500, and T2000) obtained from Pharmacia Fine Chemicals (Uppsala, Sweden) were used without further purification. T3500 was prepared by fractionating T2000 in a standard procedure.⁸ Their molecular weights are moderately distributed ($\bar{M}_w/\bar{M}_n = 1.5$ – 2.5) except that of T2000. These dextrans were prepared by fractionating material synthesized from sucrose by the bacterial species *Leuconostoc mesenteroides* strain B512. The branching points of dextran produced in this way are about 5% of the degree of polymerization.⁹ Doubly distilled, deionized water was used as solvent. The water content in these samples has been determined to be $\sim 10\%$, which was taken into account when we calculated the final dextran concentration, which ranged from 0.1 to 4 g/L depending on M_w . All solutions were clarified with a 0.22- μm Millipore filter in order to remove dust.

Laser Light Scattering. A commercial LLS spectrometer (ALV/SP-86, Langen in Hessen, Germany) was used with an argon ion laser (Coherent INNOVA 300, operated at wavelength 488 nm and 300 mw) as the light source. The primary beam is vertically polarized. By placing a polarizer in front of the detector, we measured only the vertically polarized scattered light. An ALV 3000 correlator with 240 linear channels was used to measure the intensity–intensity time correlation functions. Laser light scattering instrumentation and its operation can be found elsewhere.¹⁸ All measurements were performed at $25.0 \pm 0.1^\circ\text{C}$.

4. Results and Discussion

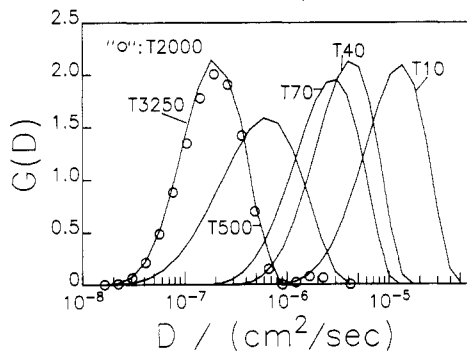
Our laser light scattering results together with the gel filtration results supplied with the samples by Pharmacia Fine Chemicals are summarized in Table I. We will discuss the results of T2000 and T3250 later. It can be seen that the agreements between M_w s obtained by these two different methods are rather satisfactory, except for T70. Our repeated measurements and the experiments in our other laser light scattering laboratory confirm that M_w of T70 is ~ 65 000. The second virial coefficient of dextran decreases sharply as the molecular weight increases. This

Table I. Static and Dynamic Light Scattering Results of Dextrans

	T10	T40	T70	T500	T2000	T3250
$M_w/(10^4)$	0.99	3.97	6.50	48.1	227	325
$A_2/(10^{-3} \text{ mL}\cdot\text{mol}/\text{g}^2)$	1.38	0.92	0.77	0.39	0.09	0.07
$\langle R_g^2 \rangle_z^{1/2}/\text{nm}$				23	46	48
$\bar{D}/(10^{-7} \text{ cm}^2/\text{s})$	9.10	4.39	3.32	1.40	0.74	0.66
$k_d/(\text{mL}/\text{g})$	~ 10	~ 10	~ 10	~ 20	~ 60	~ 90
f	0.13	0.09	0.07	0.05	0.06	0.05
$\langle R_g^2 \rangle_z^{1/2}/R_h$				1.3	1.4	1.3

Gel Filtration Data Provided by Pharmacia Fine Chemicals

$M_w/(10^4)$	0.97	3.99	7.03	48.7
M_w/M_n	1.62	1.60	1.85	2.69

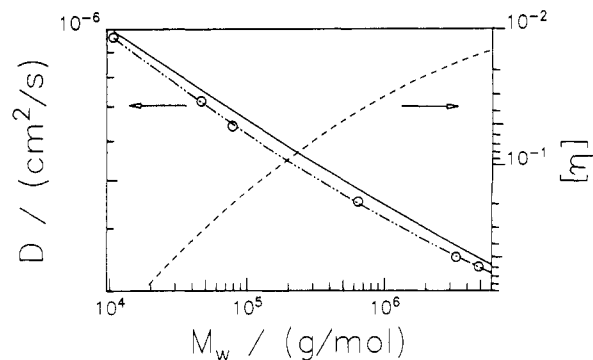
**Figure 3.** Translational diffusion coefficient distributions of six dextran samples measured in water at 25 °C, where $C \rightarrow 0$ and $q \rightarrow 0$.

suggests that high molecular weight dextrans have more densely filled conformations because their branching densities are higher. The molecular sizes of T10, T40, and T70 are so small that the scattering intensities are virtually independent of the scattering angle. Therefore, it is impossible to determine the exact values of $\langle R_g^2 \rangle_z^{1/2}$ by using laser light scattering. Due to the branching, the measured $\langle R_g^2 \rangle_z^{1/2}$ and f values of dextrans are smaller than the ones of a linear flexible polymer with a similar number of Kuhn segments in good solvent.^{23,24} The values of $\langle R_g^2 \rangle_z^{1/2}$ and \bar{D} are similar to those listed in the literature.^{10,25}

Figure 3 shows six translational diffusion coefficient distributions of dextran in water at 25 °C. It should be stated that, in the process of reducing $G(T)$ to $G(D)$, we have used \bar{k}_d and \bar{f} instead of k_d and f , respectively, because both $1 + k_d C$ and $1 + f \langle R_g^2 \rangle_z q^2$ are very small in our present experiments. It can be seen in Figure 3 that all distributions except T2000 are monomodal. T2000 is very broadly distributed and has a bimodal distribution. This is why we have to fractionate it in order to obtain a sample (T3500) with a narrower MWD and a higher M_w . In order to transform those $G(D)$ s in Figure 3 into $F_w(M)$ or $F_n(M)$, we encountered the following two problems:

The first problem is that the branching density of dextran increases as a function of molecular weight, resulting in more compact molecules, which means $D \neq k_D M^{-\alpha_D}$ or the plot of $\log D$ versus $\log M$ is not a straight line. The second problem is that a set of narrowly distributed dextran standards is not available so that we were not able to use the measured \bar{D} and M_w as D and M , respectively, in the calibration.

Figure 4 shows a log-log plot of \bar{D} versus M_w , where \bar{D} was calculated from $G(D)$ in Figure 3. However, the data points do not follow a straight line. The question is whether this curvature is due to polydispersity and experimental uncertainty or due to the change of branching density as a function of molecular weight. In order to answer this question, let us look at some intrinsic viscosity

**Figure 4.** Double-logarithmical plot of \bar{D} versus M_w (circles). The dot-dashed line shows a least-squares fit of $\log \bar{D} = \log(6.51 \times 10^{-4}) - 0.876 \log M_w + 4.02 \times 10^{-2} (\log M_w)^2$. The solid line represents a calibration between D and M , where $\log D = \log(1.98 \times 10^{-4}) - 0.657 \log M + 2.01 \times 10^{-2} (\log M)^2$. The dashed line shows how intrinsic viscosity $[\eta]$ changes as a function of M_w , calculated from the data presented in ref 8.

($[\eta]$) data, which are related to hydrodynamic size in a similar way as D , because the plot of $\log [\eta]$ versus $\log M$ should be more curved if the curvature is intrinsic.²⁶ The dashed line in Figure 4 shows a fit of $\log [\eta] = \log(2.62 \times 10^{-5}) + 1.22 \log M_w - 8.12 \times 10^{-2} (\log M_w)^2$, which was calculated from the data listed in ref 8. After realizing that the curvature in the plot of $\log D$ versus $\log M$ is intrinsic, we decided to use the following empirical equation to fit our data in Figure 4:

$$\log D = \log k_D - \alpha_D' \log M + \alpha_D'' (\log M)^2 \quad (8)$$

The broken line in Figure 4 represents a least-squares fitting of eq 8 with $\bar{k}_D = 6.51 \times 10^{-5}$, $\bar{\alpha}_D' = 0.876$, and $\bar{\alpha}_D'' = 4.02 \times 10^{-2}$ where bars over these parameters mean that they are obtained from \bar{D} and M_w instead of from D and M . It is interesting to note that $d \log [\eta] / d \log M \approx 3(d \log D / d \log M) - 1$ when $M_w \sim 2 \times 10^5$ (in the middle of the curves), which is very close to Flory's prediction.²⁶

By using eqs 7 and 8 with $\bar{k}_D = 6.51 \times 10^{-5}$, $\bar{\alpha}_D' = 0.876$, and $\bar{\alpha}_D'' = 4.02 \times 10^{-2}$, we were able to calculate $F_w(M)$ and $F_n(M)$. In order to have a direct comparison with our static light scattering results, we need to calculate M_w and M_n from $F_w(M)$ and $F_n(M)$, respectively, according to their definitions,

$$(M_w)_{\text{calcd}} = \frac{\int_0^\infty F_w(M) M dM}{\int_0^\infty F_w(M) dM} = \frac{\int_0^\infty G(D) dD}{\int_0^\infty G(D)/M dD} \quad (9)$$

and

$$(M_n)_{\text{calcd}} = \frac{\int_0^\infty F_n(M) M dM}{\int_0^\infty F_n(M) dM} = \frac{\int_0^\infty G(D)/M dD}{\int_0^\infty G(D)/M^2 dD} \quad (10)$$

The weight- and number-average molecular weights calculated with \bar{k}_D , $\bar{\alpha}_D'$, and $\bar{\alpha}_D''$ are listed in Table II. It is not a surprise to find that M_w and M_w/M_n calculated in this way are smaller than the ones obtained by using static LLS and gel filtration because we have used \bar{k}_D , $\bar{\alpha}_D'$, $\bar{\alpha}_D''$ instead of k_D , α_D' , and α_D'' , respectively. It is known that \bar{k}_D , $\bar{\alpha}_D'$ calculated from a set of broadly distributed samples are usually different from k_D , α_D' , and α_D'' obtained from a set of monodisperse standards (or very narrowly distributed samples).¹⁶ On the basis of this failed trial, we decided to solve the above two problems simultaneously by using the following principle:

For N -number samples, we have N -number measured M_w and $G(D)$, denoted as $M_{w,i}$ and $G_i(D)$ where $i = 1-N$.

Table II. Calculated M_w and M_w/M_n of Dextrans from $G(D)$

	T10	T40	T70	T500	T2000	T3250
$M_w/(10^4)$	0.89	3.24	5.10	30.6	148	200
M_w/M_n	1.46	1.51	1.63	2.20	5.77	2.08
using eq 8 with $k_D = 6.51 \times 10^{-4}$, $\alpha_D' = 0.876$, and $\alpha_D'' = 0.0402$						
using $\log D = \log k_D - \alpha_D'$ $\log M + \alpha_D'' (\log M)^2$ where $k_D = 1.90 \times 10^{-4}$, $\alpha_D' = 0.659$, and $\alpha_D'' = 2.09 \times 10^{-2}$						
$M_w/(10^4)$	0.96	4.10	6.75	46.6	233	312
M_w/M_n	1.59	1.63	1.77	2.38	6.16	2.07
using eq 8 with $k_D = 1.90 \times 10^{-4}$, $\alpha_D' = 0.659$, and $\alpha_D'' = 0.0209$						

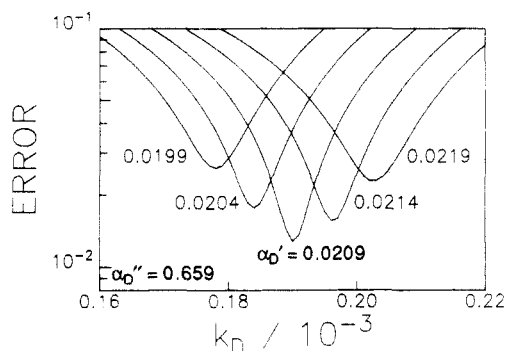


Figure 5. Typical plot of ERROR versus k_D with different α_D'' but a fixed $\alpha_D' = 0.659$, where the overall minimum is located at $\alpha_D'' = 2.09 \times 10^{-2}$ and $k_D = 1.90 \times 10^{-4}$.

By assuming a set of k_D , α_D' , and α_D'' in eq 8 and using eq 9, we are able to calculate N -number (M_w)_{calcd}, denoted as $(M_{w,i})_{\text{calcd}}$ where $i = 1-N$. In principle, $(M_{w,i})_{\text{calcd}}$ should equal $M_{w,i}$ if k_D , α_D' , and α_D'' are correctly chosen. Therefore, our object is to find a set of k_D , α_D' , and α_D'' which can minimize the ERROR defined as

$$\text{ERROR} = \frac{1}{N} \sum_{i=1}^N \left[\frac{M_{w,i} - (M_{w,i})_{\text{calcd}}}{M_{w,i}} \right]^2 \quad (11)$$

It is clear that this procedure is an M_w -constrained analysis. In this way, by using eq 8 instead of $D = k_D M^{-\alpha_D}$, we have taken into account the conformation change as a function of molecular weight; and by using k_D , α_D' , and α_D'' instead of \bar{k}_D , $\bar{\alpha}_D'$, and $\bar{\alpha}_D''$, we have avoided the polydispersity problem.

Figure 5 shows a typical plot of ERROR versus k_D with different α_D'' but a fixed $\alpha_D' = 0.659$. It can be seen in Figure 5 that there is a minimum ERROR for each given α_D'' and there is an overall minimum for a fixed α_D' . Figure 6 shows a similar plot of ERROR versus k_D with different α_D' but a fixed $\alpha_D'' = 2.09 \times 10^{-2}$. There is also an overall minimum for a fixed α_D'' . Therefore, by combining Figures 5 and 6, we know there exists a set of k_D , α_D' , and α_D'' which corresponds to an overall minimum point on the ERROR surface. Numerically, we were able to find this overall minimum at $k_D = 1.90 \times 10^{-4}$, $\alpha_D' = 0.659$, and $\alpha_D'' = 2.09 \times 10^{-2}$, which defines a calibration between D and M . The continuous line in Figure 4 represents such a calibration. Its obvious deviation from our measured \bar{D} and M_w clearly shows how serious error could be introduced in practice if we would use \bar{D} and M_w measured from a set of broadly distributed samples instead of D and M . However, from the experimental point of view, this overall minimum point is not well-defined because there is always

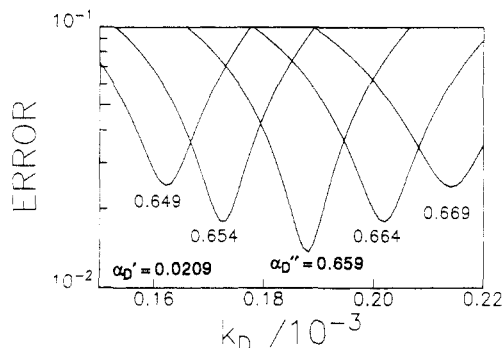


Figure 6. Typical plot of ERROR versus k_D with different α_D' but a fixed $\alpha_D'' = 2.09 \times 10^{-2}$, where the overall minimum is located at $\alpha_D' = 0.659$ and $k_D = 1.90 \times 10^{-4}$.

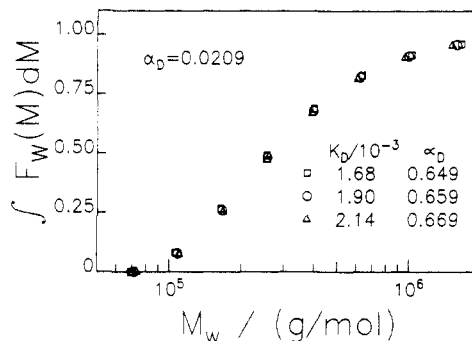


Figure 7. Comparison of three cumulative weight distributions of dextran T500. They were calculated from $G(D)$ with three different sets of k_D and α_D' but a fixed $\alpha_D'' = 2.09 \times 10^{-2}$.

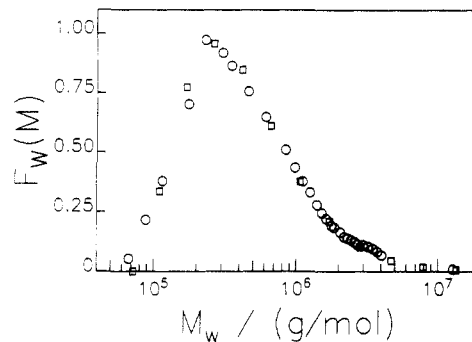


Figure 8. Comparison of two molecular weight distributions of dextran T500: (O) $F_w(M)$ calculated from $G(D)$ by using eqs 7 and 8 with $k_D = 1.90 \times 10^{-4}$, $\alpha_D' = 0.659$, and $\alpha_D'' = 2.09 \times 10^{-2}$; (□) $F_w(M)$ from gel filtration.

some experimental noise in both M_w and $G(D)$. The important question is how much error this uncertainty will introduce into the final molecular weight distributions.

Figure 7 shows three cumulative weight distributions of T500 calculated with three different sets of k_D , α_D' , and α_D'' , where we have intentionally shifted the minimums to both sides of the overall minimum. It can be seen in Figure 7 that there is no significant difference among those three distributions and some uncertainty in this overall minimum will not introduce serious errors in our calculated molecular weight distribution.

Figure 8 shows a comparison between $F_w(M)$ calculated from $G(D)$ and $F_w(M)$ obtained by using gel filtration (supplied by Pharmacia Fine Chemicals, Uppsala, Sweden). Two distributions in Figure 8 are comparable in spite of a slight difference in the distribution width. This difference is understandable because the scattered light intensity is proportional to M^2 so that small molecules in a broad distribution cannot be "seen" by the detector. Therefore, for a broadly distributed sample, MWD ob-

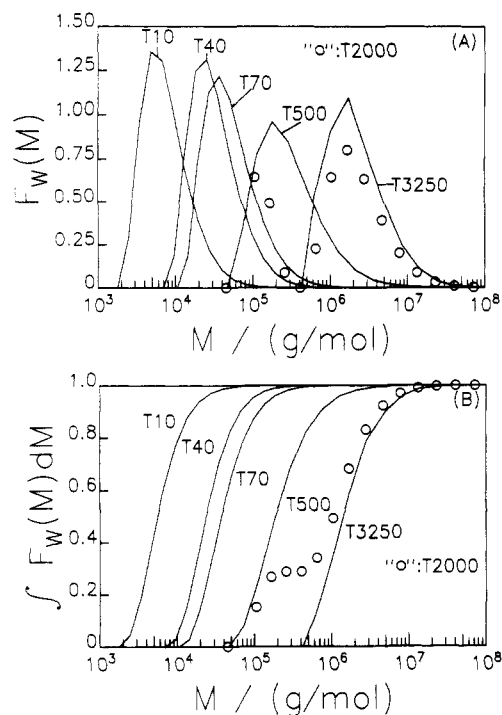


Figure 9. (A) Weight distributions calculated from $G(D)$ by using eqs 7 and 8 with $k_D = 1.98 \times 10^{-4}$, $\alpha_D' = 0.657$, and $\alpha_D'' = 2.01 \times 10^{-2}$. (B) Cumulative weight distributions calculated from $F_w(M)$ s in Figure 9A.

tained by using LLS is normally narrower than the actual one.

On the basis of the above discussion, we are confident in using this set of calculated k_D , α_D' , and α_D'' to transform $G(D)$ s in Figure 3 into $F_w(M)$ s. The calculated $F_w(M)$ and $\int_0^M F_w(M) dM$ of dextrans are shown in parts A and B of Figure 9, respectively. The calculated M_w and M_w/M_n from $F_w(M)$ and $F_n(M)$ are also listed in Table II. They essentially agree with those values obtained from the static light scattering and gel filtration experiments if we take account of all experimental noises in these three different experiments.

5. Conclusions

We demonstrate, for the first time, that the molecular weight distribution of dextran with different branching densities can be characterized by only using one analytical method of laser light scattering. A calibration between the translational diffusion coefficient and the molecular weight of dextran in water at 25 °C is established, which is independent of our particular LLS instrument; i.e., it can be used in future LLS experiments as long as water is used as the solvent and the solution temperature is 25

°C. In the calibration process, we have shown the problems of the change of the branching density as a function of molecular weight and the lack of a set of dextran standards can be solved by using a new M_w -constrained analysis. This analysis procedure should be valuable for characterizing other special systems where the polymer conformation changes as a function of molecular weight or a set of narrowly distributed standards with different molecular weights is not available.

Acknowledgment. The author thanks all his colleagues, especially Drs. Horn and Lüddecke, for their hospitality when he was in BASF, Mr. Kern for helping with the experiments, and Mr. Werle for preparing the figures.

References and Notes

- (1) Jeanes, A.; Wilham, C. A.; Mier, J. C. *J. Biol. Chem.* **1948**, *176*, 603.
- (2) Sloan, J. W.; Alexander, B. H.; Lohmar, R. L.; Wolff, I. A.; Rist, C. E. *J. Am. Chem. Soc.* **1954**, *76*, 4429.
- (3) Van Cleve, J. W.; Schaefer, W. C.; Rist, C. E. *J. Am. Chem. Soc.* **1956**, *78*, 4435.
- (4) Bixler, G. H.; Hines, G. E.; McGhee, R. M.; Churter, R. A. *Ind. Eng. Chem.* **1954**, *46*, 370.
- (5) Howell, J. A. *J. Macromol. Sci. Chem.* **1974**, *A8* (4), 725 and references therein.
- (6) Basedow, A.; Ebert, K. H.; Ederer, H.; Hunger, H. *Makromol. Chem.* **1976**, *177*, 1501 and references therein.
- (7) Wan, P. J.; Adams, E. T., Jr. *Polym. Prepr. (Am. Chem. Soc., Div. Polym. Chem.)* **1974**, *15* (1), 509.
- (8) Senti, F. R.; Hellman, N. N.; Ludwig, N. H.; Babcock, G. E.; Tobin, R.; Glass, C. A.; Lamberts, B. L. *J. Polym. Sci.* **1955**, *17*, 527.
- (9) Burchard, W.; Pfannemüller, B. *Makromol. Chem.* **1969**, *121*, 18.
- (10) Sellen, D. B. *Polymer* **1975**, *16*, 561.
- (11) Koppel, D. E. *J. Chem. Phys.* **1972**, *57*, 4814.
- (12) Provencher, S. W. *Biophys. J.* **1976**, *16*, 29; *J. Chem. Phys.* **1976**, *64*, 2772; *Makromol. Chem.* **1979**, *180*, 201.
- (13) Langowski, J.; Bryan, R. *Prog. Colloid Polym. Sci.* **1990**, *81*, 269.
- (14) Morrison, I. D.; Grabowski, E. F. *Langmuir* **1985**, *1*, 496.
- (15) Wu, C.; Zuo, J.; Chu, B. *Macromolecules* **1989**, *22* (2), 633.
- (16) Chu, B.; Wu, C.; Buck, W. *Macromolecules* **1989**, *22* (2), 831.
- (17) Zimm, B. H. *J. Chem. Phys.* **1948**, *16*, 1099.
- (18) Chu, B. *Laser Light Scattering*; Academic Press: New York, 1974.
- (19) Pecora, R. *Dynamic Light Scattering*; Plenum Press: New York, 1976; p 217.
- (20) Stockmayer, W. H.; Schmidt, M. *Pure Appl. Chem.* **1982**, *54*, 407; *Macromolecules* **1984**, *17*, 509.
- (21) Chu, B.; Wu, C.; Ford, J. R. *J. Colloid Interface Sci.* **1985**, *105*, 473.
- (22) Pope, J. W.; Chu, B. *Macromolecules* **1984**, *17*, 2633.
- (23) Chu, B.; Wu, C. *Macromolecules* **1987**, *20*, 93 (Figure 9 and references therein).
- (24) Burchard, W. *Adv. Polym. Sci.* **1983**, *48*, 1 (Chapter D.III).
- (25) Ebert, K. H.; Brosche, M. *Biopolymers* **1967**, *5*, 423.
- (26) Flory, P. J. *Principles of Polymer Chemistry*; Cornell University Press: Ithaca, NY, 1953.